催化学报
2011 Chinese Journal of Catalysis Vol. 32 No. 7

文章编号: 0253-9837(2011)07-1156-10 国际版 DOI: 10.1016/S1872-2067(10)60234-3 研究论文: 1156~1165

超声浸渍对费托合成 $Co/Zr/SiO_2$ 催化剂性能的影响

周晓峰[1,*], 陈庆龄[2], 陶跃武[2], 翁惠新[1]

[1]华东理工大学化工学院石油加工研究所, 上海 200237

[2]中国石化上海石油化工研究院, 上海 201208

摘要: 采用超声浸渍法制备了费托合成 $Co/Zr/SiO_2$ 催化剂, 考察了超声波功率对催化剂费托反应性能的影响, 并运用 N_2 物理吸附、X 射线衍射、H_2 程序升温脱附、H_2 程序升温还原和透射电子显微镜对催化剂进行了表征. 结果表明, 超声波处理可以增大催化剂的比表面积, 减小金属 Co 的粒径, 并使其较为均匀地分散于载体表面, 其中以高功率超声波作用最为显著; $Co(NO_3)_2$ 水溶液在高功率超声波场中, 随着超声时间的延长, 溶液 pH 值降低, 使得 Co–SiO_2 相互作用减弱, 抑制了硅酸钴的生成. 经高功率超声波处理的催化剂, 活性金属 Co 在载体上分散度和还原度较高, 因而催化剂的活性和稳定性较高. 在 493 K, 2 MPa, H_2/CO = 2.0 和 GHSV = 1000 h^{-1} 反应条件下, CO 初始转化率可达 95.5%, 反应 48 h 时, CO 转化率为 90.9%.

关键词: 费托合成; 超声浸渍; 真空; 钴; 锆; 氧化硅

中图分类号: O643 **文献标识码**: A

收稿日期: 2011-02-16. 接受日期: 2011-03-16.

*通讯联系人. 电话: (021)68462197-5402; 传真: (021)68462283; 电子信箱: zhouxiaofeng2002@163.com

本文的英文电子版(国际版)由Elsevier出版社在ScienceDirect上出版(http://www.sciencedirect.com/science/journal/18722067).

Influence of Ultrasound Impregnation on the Performance of $Co/Zr/SiO_2$ Catalyst during Fischer-Tropsch Synthesis

ZHOU Xiaofeng[1,*], CHEN Qingling[2], TAO Yuewu[2], WENG Huixin[1]

[1]*Research Center of Petroleum Processing, East China University of Science and Technology, Shanghai 200237, China*

[2]*Shanghai Research Institute of Petrochemical Technology, SINOPEC, Shanghai 201208, China*

Abstract: A $Co/Zr/SiO_2$ catalyst for Fischer-Tropsch synthesis was prepared under an ultrasound environment. The influence of different ultrasonic powers on catalyst performance was studied. The catalysts were characterized by N_2 physisorption, X-ray diffraction, H_2 temperature-programmed desorption, H_2 temperature-programmed reduction, and transmission electron microscopy. The results show that ultrasound assisted in increasing the BET surface area of the catalysts and the even the dispersion of small cobalt crystallites on the support. When higher power ultrasound was used these characteristics of the catalyst changed remarkably. The pH of the $Co(NO_3)_2$ aqueous solution decreased with an increase in high power ultrasound treatment time, which led to a weak interaction between the smaller cobalt particles and the silica support. In addition, less cobalt silicate was formed on the catalyst. Under the same reaction conditions, the catalyst activity and stability were superior to that of the other catalysts because of higher dispersion and reduction. For example, the initial conversion of CO was 95.5% at 493 K, 2 MPa, H_2/CO = 2.0, and GHSV = 1000 h^{-1}, and it was 90.9% after 48 h.

Key words: Fischer-Tropsch synthesis; ultrasound impregnation; vacuum; cobalt; zirconium; silica

Received 16 February 2011. Accepted 16 March 2011.

**Corresponding author. Tel: +86-21-68462197-5402; Fax: +86-21-68462283; E-mail: zhouxiaofeng2002@163.com*

English edition available online at Elsevier ScienceDirect (http://www.sciencedirect.com/science/journal/18722067).

随着石油资源的日益枯竭及其消费的日益增长, 人们逐渐意识到寻找石油替代能源的重要性. 以煤或天然气为原料制得合成气, 再经费托合成 (FTS) 反应制低碳烯烃、汽油、柴油及石蜡烃的工艺路线, 在一定程度上可以缓解人们对于石油的依赖性. 费托 Fe, Co 基催化剂已成功应用于 Sasol 公司和 Shell

公司的工业化装置. 与Fe基催化剂相比, Co基催化剂上水煤气反应活性较低, 性能较为稳定, 在合成长链正构烷烃方面具有较大优势[1~3].

近年来, 国内科研机构在Co基催化剂研发及工业化进程中取得了一定的成绩. 2007年, 中科院大连化学物理研究所研制的Co基催化剂进行3000吨/年中试试验, 催化剂连续稳定运行了5000 h (中科院大连化学物理研究所60年重大科技成果和优势发展学科. 2009-02); 2010年, 中科院山西煤炭化学研究所研制的Ⅰ型Co基催化剂, 经过实验室长周期评价和单管试验, 目前已实施了5000吨级工业侧线[4,5]; 2010年, 中国石化石油化工科学研究院开发的RFT-2催化剂进行中试试验, 该催化剂可在高空速、高转化率条件下稳定运行[6].

SiO_2负载的Co基催化剂一般采用常温常压浸渍法制备. Zr助剂的添加可减弱Co/SiO_2催化剂中Co与载体间的相互作用, 有利于金属Co的还原, 从而提高催化剂活性和重质烃的选择性[3]. 但是, 在干燥和焙烧过程中, 负载于载体表面的Co_3O_4晶粒容易聚集形成较大颗粒, 从而最终降低金属Co的分散度, 而金属颗粒在载体表面大小及其分布的均匀性将影响催化剂的催化性能及稳定性[7~9]. 因此, 改善活性金属Co在载体表面的分散性成为Co/Zr/SiO_2催化剂研究的重点.

超声浸渍是指在催化剂制备过程中, 将浸渍体系置于超声波场, 浸渍液在高温高压下会产生空化气泡, 利用这些气泡溃陷时所产生的高速射流束, 将活性组分负载于载体表面[10]; 同时利用超声波的机械振荡效应, 使组分得到均匀分散[11,12]. 文献[13~15]将不同的活性组分通过超声浸渍方法负载于γ-Al_2O_3上, 与普通浸渍法相比, 超声浸渍除了可以减小金属晶粒的粒径, 增大催化剂的比表面积以外, 还可以使活性组分均匀分散于载体上, 从而提高催化剂的活性和稳定性. 文献[16,17]通过超声浸渍分别将Fe和Co负载于SiO_2载体, 发现活性金属晶粒在载体表面分散度较高, 在费托合成反应中CO转化率和稳定性较高.

一般认为, 当超声波频率一定时, 超声波强度增加, 其空化效应增强[10]. 系统压力提高, 一方面, 可以使部分气体溶解于液体溶剂中, 空化阈(液体介质产生空化作用的最低声强或是声压振幅)降低; 另一方面, 液体溶剂中所含气体组分以及溶剂蒸气压增加, 导致空化气泡溃陷时产生的冲击波强度降低, 不利于空化作用[10,18]. 因此, 综合考虑并根据真空超声波清洗原理[19], 将超声浸渍体系置于真空环境中, 对浸渍液进行脱气处理, 避免溶剂自身的影响, 从而强化超声浸渍过程.

目前尚未见有关超声浸渍用于制备费托合成Co/Zr/SiO_2催化剂的报道. 本文采用真空-超声浸渍法制备费托Co基催化剂, 在超声波频率一定的条件下, 考察超声波功率对制得催化剂的结构、Co晶粒尺寸、分散性、还原性及其催化费托合成性能的影响, 并用N_2物理吸附、X射线衍射(XRD)、H_2程序升温脱附(H_2-TPD)、H_2程序升温还原(H_2-TPR)和透射电子显微镜(TEM)表征催化剂, 以期为提高Co/Zr/SiO_2催化剂中Co的分散度提供参考.

1 实验部分

1.1 催化剂的制备

将SiO_2载体(国药集团化学试剂有限公司)放入超声波发生器中(Branson公司, 超声波频率42 kHz, 有效功率180和210W), 在真空(–0.1 MPa)条件下, 用5% $Zr(NO_3)_4$(AR, 国药集团化学试剂有限公司)水溶液等体积浸载体, 开启超声波发生器超声1 h. 催化剂前体在383 K干燥12 h后, 在真空(–0.1 MPa)条件下等体积浸入20% $Co(NO_3)_2$(AR, 国药集团化学试剂有限公司)水溶液, 开启超声波发生器处理1 h. 催化剂在383 K干燥12 h, 673 K焙烧6 h. 然后经压片、粉碎、筛分, 取60~80目的颗粒备用. 将上述制得的催化剂分别标记为20%Co/5%Zr/SiO_2(H)和20%Co/5%Zr/SiO_2(L). 其中H和L分别代表高和低功率超声浸渍. 为了比较, 不经超声波处理, 采用真空浸渍法制得20%Co/5%Zr/SiO_2(V)催化剂.

另外, 分别将20% $Co(NO_3)_2$和5% $Zr(NO_3)_4$水溶液置于不同功率的超声波场中, 考察超声时间对溶液pH值的影响. pH值用上海精密科学仪器有限公司PHSJ-3F型pH计(分辨率0.01)测量, 使用前先用pH值为4.0和7.0的标准缓冲溶液校正.

1.2 催化剂的表征

催化剂的比表面积测定在Micromeritics公司ASAP 2010型物理吸附仪上进行. XRD测试在德国Bruker公司D8-ADVANCE型X射线衍射仪上进行,

Cu K_α射线, 管压 40 kV, 管流 40 mA, 扫描速率 4°/min. H_2-TPR 实验在 Micromeritics 公司 Autochem Ⅱ2920 型化学吸附仪上进行, 样品用量 50 mg, 通入 10% H_2-90% Ar 混合气 (50 ml/min) 进行程序升温, 升温速率 10 K/min. H_2-TPD 实验在自建装置上进行, 催化剂先用纯 H_2 在 673 K 还原 5 h, 降至室温再用高纯 N_2 (30 ml/min) 吹扫 1 h, 以 10 K/min 升温至 1073 K. 样品形貌在 FEI Tecnai 20 S-TWIN 型 TEM 上观测.

1.3 催化剂的评价

费托合成反应在固定床微反装置 (φ 8 mm) 上进行. 催化剂用 H_2 在常压 673 K 下还原 12 h 后, 降到室温, 切换为合成气, 逐渐升压到设定值; 同时, 以 2 K/min 升温到设定值. 当反应达到稳定状态 (反应进行 12 h) 后, 取样分析, 计算 CO 转化率和烃类选择性. 其中, 气相产物用 Agilent 6890(N) 型气相色谱在线分析, 液相产物用 Agilent 6820 型气相色谱离线分析.

2 结果与讨论

2.1 催化剂的织构和物相

表 1 为不同 Co/Zr/SiO_2 催化剂样品的物性数据. 活性组分的负载使得载体的比表面积、孔体积和平均孔径减小. 当浸渍处于高功率超声波场时, 催化剂的比表面积相对较大. 这与文献[13~16]结果一致.

在各催化剂的 XRD 谱 (图略) 中均未发现 Zr 物相, 说明 ZrO_2 高度分散于载体上[7]. 根据文献[20~22], Co_3O_4 的平均粒径可根据 $2\theta = 36.9°$ 处衍射峰, 利用 Scherrer 公式进行计算; 金属 Co 的平均粒径 d 和分散度 D 分别按照公式 $d = 0.75 \times d(Co_3O_4)$ 及 $D(\%) = 96/d$ 计算. 由表 1 可以看出, 用高功率超声波处理后的 20%Co/5%Zr/SiO_2(H) 催化剂中, Co 晶粒明显减小, 导致 Co 分散度提高.

图 1 为不同 Co/Zr/SiO_2 催化剂样品的 TEM 照片. 由图可见, 未经超声波处理的 20%Co/5%Zr/SiO_2(V) 催化剂表面上 Co 颗粒分散杂乱; 经超声波处理后, Co_3O_4 颗粒分散趋于均匀, 其中在高功率超声波场中, Co_3O_4 颗粒呈现云雾状态, 说明 Co 颗粒较小且分散度较高. 这与梁新义等[13]发现超声波场可以促进 $LaCoO_3$ 在 γ-Al_2O_3 载体上均匀分散的现象一致. 另外, Zr 和 Co 盐溶液在真空中浸渍硅胶载体, 在超声波场中溶液依然具有“空化效应”, 会产生空化气泡. 由图 1(d) 可见, 20%Co/5%Zr/SiO_2(H) 催化剂表面经过空化气泡刻蚀后遗留下了气泡痕迹.

2.2 超声波对浸渍溶液 pH 值的影响

超声波所产生的高温高压环境可以改变盐溶液

表 1 不同 Co/Zr/SiO_2 催化剂样品的织构性质和 Co 颗粒大小

Table 1 Textural properties and Co particle size of different Co/Zr/SiO_2 samples

Sample	Surface area (m^2/g)	Pore volume (cm^3/g)	Average pore diameter (nm)	Average particle size (nm)		Dispersion degree (D/%)	Reduction degree[a] (%)
				Co_3O_4	Co		
SiO_2	191.5	0.3	7.9	—	—	—	—
20%Co/5%Zr/SiO_2(V)	125.2	0.2	7.2	22.2	16.6	5.8	52.3
20%Co/5%Zr/SiO_2(L)	125.3	0.2	7.0	21.8	16.3	5.9	55.9
20%Co/5%Zr/SiO_2(H)	129.5	0.2	6.9	19.8	14.8	6.5	59.1

[a]The reduction degree was calculated on the basis of H_2 consumption in the TPR experiments from 473 to 1000 K.
V—vacuum impregnation; L—ultrasound impregnation with lower power (180 W); H—ultrasound impregnation with higher power (210 W).

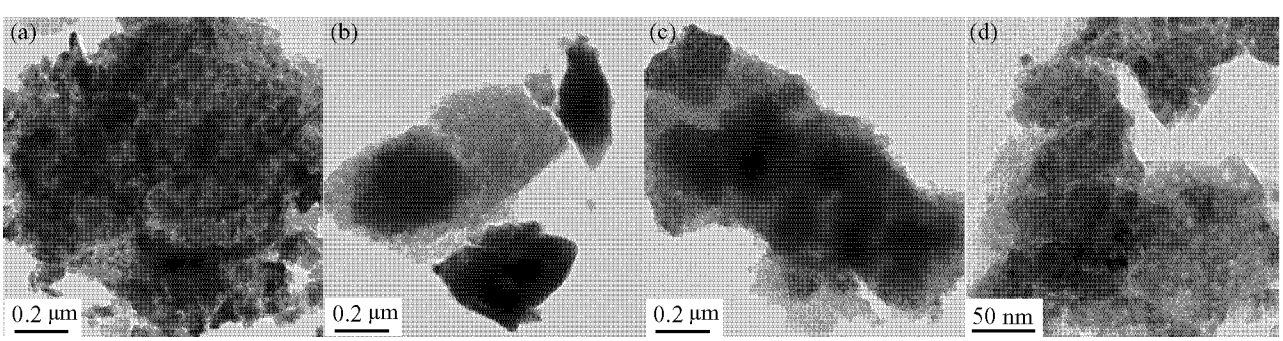

图 1 不同 Co/Zr/SiO_2 催化剂样品的 TEM 照片

Fig. 1. TEM images of different Co/Zr/SiO_2 catalyst samples. (a) 20%Co/5%Zr/SiO_2(V); (b) 20%Co/5%Zr/SiO_2(L); (c), (d) 20%Co/5%Zr/SiO_2(H).

的 pH 值. 表 2 为 20% $Co(NO_3)_2$ 和 5% $Zr(NO_3)_4$ 水溶液在不同功率的超声波场中处理不同时间的 pH 值. 两种溶液在高功率超声波场中 pH 值降低幅度较大. 其中 $Co(NO_3)_2$ 溶液经高功率超声 1 h 后, 溶液中出现粉红色 $Co(OH)_2$ 沉淀物. 这是因为水溶液在高强度超声波中生成更多的 $H^{\bullet}$ 和 $OH^{\bullet}$ 自由基[10], 使得水合 $Co(H_2O)_6^{2+}$ 离子与 $OH^{\bullet}$ 自由基反应生成难溶解的 $Co(OH)_2$ 沉淀物 (水合 Co^{3+} 离子氧化性很强, 在水溶液中不能存在[23]), 从而使得溶液的 pH 值明显降低. 而低功率超声波对溶液 pH 值的影响不太明显.

表 2 浸渍溶液在不同功率超声波场中的 pH 值

Table 2 pH values of the impregnation solution within different ultrasound circumstance

Impregnation solution	Initial	pH			
		210 W		180 W	
		0.5 h	1.0 h	0.5 h	1.0 h
20% $Co(NO_3)_2$	3.31	3.16	3.00	3.26	3.19
5% $Zr(NO_3)_4$	0.95	0.85	0.83	0.90	0.88

陈建刚等[24]认为, 在浸渍过程中, $Co(H_2O)_6^{2+}$ 与硅胶表面羟基发生类似氢键的相互作用. 硅胶是两性材料, 表面 Si–OH, SiO^- 及 $SiOH_2^+$ 的相对数量与浸渍溶液的 pH 有关. Van Steen 等[25]认为, 浸渍液 pH 值越高, $Co(H_2O)_6^{2+}$ 与硅胶表面硅羟基的相互作用越强, 并且通过氧桥形成硅酸钴; 同时, $Co(H_2O)_6^{2+}$ 中配体 H_2O 分子的数量有助于硅酸钴的形成. 文献[26~28]也认为, 浸渍液 pH 值影响 Co 与载体间的相互作用, 当浸渍液 pH 值低于硅胶的等电点 (2.0~3.5[29]) 时, 硅胶表面带正电, 直接吸附带负电的 NO_3^-, 然后再通过静电作用吸附 $Co(H_2O)_6^{2+}$. 以这种方式吸附到硅胶表面上的 Co 与硅胶相互作用较弱, 有利于提高催化剂的还原度. 高功率超声波可以显著降低浸渍溶液的 pH 值, 故理论上 20%Co/5%Zr/SiO_2(H) 催化剂中 Co 与硅胶间的相互作用较弱. 此外, 高功率超声波可以将 H_2O 分子解离为更多的 $H^{\bullet}$ 和 $OH^{\bullet}$ 自由基, 减少 $Co(H_2O)_6^{2+}$ 中配体 H_2O 分子的数目, 从而不利于硅酸钴的形成.

2.3 H_2-TPD 结果

图 2 为不同 $Co/Zr/SiO_2$ 催化剂样品的 H_2-TPD 谱. 根据文献[30], 低温峰 (约 463 K) 为从金属 Co 到载体的氢溢流; 中温峰 (约 603 K) 及高温峰 (约 703 K) 对应因载体诱导效应, 位于 ZrO_2 和 SiO_2 界面上活性中心的 H_2 脱附. 由图 2 可见, 经不同功率超声波处理后, 催化剂低温 (453 K) 峰向低温方向移动, H_2 吸附量下降; 高功率超声波使得位于 SiO_2 界面上活性中心的 H_2 脱附峰向低温移动, 并且使得位于 ZrO_2 和 SiO_2 界面上金属 Co 的 H_2 吸附量增加 (由 489~803 K 谱峰积分面积得到各催化剂上 H_2 脱附量的大小顺序为 20%Co/5%Zr/SiO_2(H) > 20%Co/5%Zr/SiO_2(L) > 20%Co/5%Zr/SiO_2(V)).

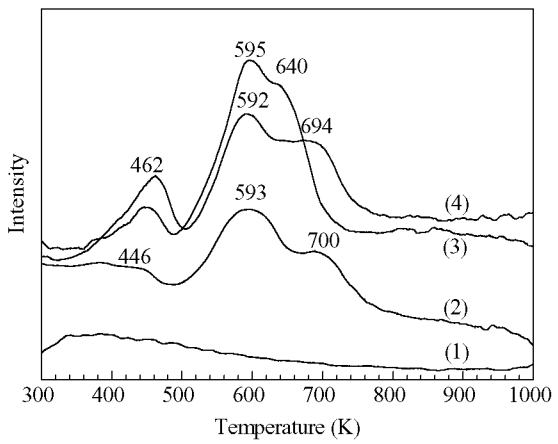

图 2 不同 $Co/Zr/SiO_2$ 催化剂样品的 H_2-TPD 谱

Fig. 2. H_2-TPD profiles of different $Co/Zr/SiO_2$ catalyst samples. (1) ZrO_2; (2) 20%Co/5%Zr/SiO_2(L); (3) 20%Co/5%Zr/SiO_2(H); (4) 20%Co/5%Zr/SiO_2(V).

Tauster 等[31]对金属与 TiO_2 载体发生强相互作用 (SMSI) 的解释为: 可还原性载体将部分电子传递给金属, 从而减弱金属对 H_2 的化学吸附能力. Ishihara 等[32]研究发现, 金属 Ru 负载于电负性较高的氧化物载体 SiO_2 上, 将会发生从金属 Ru 到载体的电子转移现象, 使得金属 Ru 电子云密度降低; 相应的 H_2-TPD 脱附峰向低温方向移动, 从而提高 CO 加氢反应活性和碳链增长能力. 对于 20%Co/5%Zr/SiO_2(H) 催化剂而言, 位于 703 K 的 H_2 脱附峰向低温移动, 有可能部分电子从金属 Co 转移到 SiO_2 载体, 导致金属 Co 的电子云密度降低, 略带正电荷, 使得 H_2 吸附峰向低温方向移动. 因此, 可以推测金属 Co 与 SiO_2 相互作用较弱, H_2 吸附量较大. 此外, 20%Co/5%Zr/SiO_2(H) 催化剂中金属 Co 的晶粒较小, 分散度较高, 同样使得该区间 H_2 的吸附量增加. 低温脱附峰向低温方向移动表明 H_2 的吸附键能变弱, 有利于 H_2 的脱附、解离以及在催化剂表面的迁移, 进而有利于费托反应的进行. 超声波对 603 K 左右位于 ZrO_2 界面上活性中心的 H_2 脱附峰峰位影响不

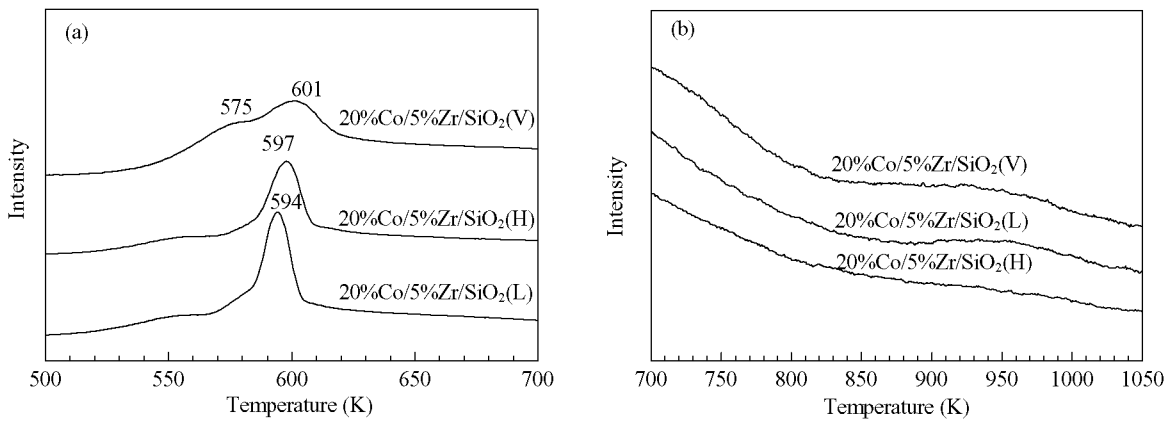

图 3 不同 Co/Zr/SiO_2 催化剂样品的 H_2-TPR 谱

Fig. 3. H_2-TPR profiles of different Co/Zr/SiO_2 catalyst samples. (a) 500–700 K; (b) 700–1050 K.

明显,表明超声波对金属 Co 与 ZrO_2 相互作用的影响较小. 这可能与 ZrO_2 含量较少有关.

2.4 H_2-TPR 结果

图 3 为不同 Co/Zr/SiO_2 催化剂样品的 H_2-TPR 谱. 一般认为, SiO_2 负载 Co 催化剂的还原过程包含 Co_3O_4 (Co^{3+}氧化物, Co^{2+}氧化物) → CoO → Co^0 两个阶段,并且在 703~1003 K 处出现 Co 与硅胶强相互作用产物硅酸钴的还原峰[2,25]. 由图可以看出, 20%Co/5%Zr/SiO_2(H) 催化剂中 Co_3O_4 的还原峰变得不明显,这与催化剂含有较少的 Co^{3+} 氧化物有关, CoO 还原峰较为尖锐,说明该温度下只有单一物种存在[26]. 20%Co/5%Zr/SiO_2(H) 催化剂的还原特性,可能与其制备时浸渍溶液处于高功率超声波场中可以生成 $Co(OH)_2$ 沉淀有关. 另外, 20%Co/5%Zr/SiO_2(H) 催化剂中硅酸钴的还原峰较小,表明高功率超声波可以减弱 Co 与硅胶的相互作用,从而抑制硅酸钴的生成.

综合 H_2-TPD 和 H_2-TPR 结果可见,高功率超声波可以减弱 Co 与硅胶相互作用,有利于提高 H_2 吸附量,从而提高催化剂中 Co 物种的还原度(见表 1); 而低功率超声波对浸渍溶液 pH 值的影响不明显, Co 与硅胶之间仍存在相互作用,导致出现硅酸钴物种.

2.5 Co/Zr/SiO_2 催化剂上费托反应性能

在 2 MPa, H_2/CO = 2.0 和 GHSV = 1000 h^{-1} 反应条件下,各 Co/Zr/SiO_2 催化剂上费托反应性能列于表 3. Iglesia[1]认为,当活性金属 Co 粒径大于 6 nm 时,费托合成是结构非敏感反应,催化剂活性与载体表面金属 Co 的数量有关,并且随着金属 Co 浓度的提高,催化剂的催化活性和 C_{5+} 选择性升高. 由上文可知,高功率超声波除了可以在载体表面均匀分散生成的较小 Co 颗粒,提高其分散度以外,还可以降低 Co 浸渍液的 pH 值,当 pH 值低于硅胶的等电点时,硅胶表面带正电荷, $Co(H_2O)_6^{2+}$ 与载体表面的硅羟基间接接触, Co-硅胶相互作用减弱,从而抑制硅酸钴的生成,

表 3 不同 Co/Zr/SiO_2 催化剂样品上费托合成反应性能

Table 3 Performance of different Co/Zr/SiO_2 catalyst samples in the Fischer-Tropsch synthesis

Sample	Temperature (K)	Conversion of CO (%)	Selectivity (%)			
			CO_2	CH_4	C_2–C_4	C_{5+}
20%Co/5%Zr/SiO_2(V)	473	53.9	1.2	13.4	16.9	68.3
	493	92.8(84.4)	6.7(4.5)	10.0(10.5)	5.6(11.5)	77.6(73.3)
	523	98.0	11.9	17.8	11.3	58.8
20%Co/5%Zr/SiO_2(L)	473	53.3	0.4	11.5	14.1	72.9
	493	92.3(84.5)	3.4(2.5)	8.6(11.0)	8.3(14.6)	79.6(71.7)
	523	99.9	10.6	14.8	11.0	63.4
20%Co/5%Zr/SiO_2(H)	473	59.9	0.3	9.6	12.9	77.0
	493	95.5(90.9)	5.3(3.6)	9.4(10.6)	4.1(10.9)	81.0(74.7)
	523	99.9	10.8	14.4	9.9	64.7

Reaction conditions: 2 MPa, H_2/CO = 2.0, GHSV = 1000 h^{-1}. The values in brackets denote the performance of the samples after a 48 h reaction.

提高其还原度, 使得20%Co/5%Zr/SiO_2(H)催化剂具有较多的反应活性中心.

此外, H_2-TPD结果表明, H_2可以在较低的温度下吸附、解离以及在催化剂表面迁移, 同样使得费托反应更容易进行. 因此在相同反应条件下, 20%Co/5%Zr/SiO_2(H)具有最高的活性和C_{5+}选择性. 另外, 各催化剂在493 K运行48 h后, 都出现不同程度的失活; 但20%Co/5%Zr/SiO_2(H)催化剂性能较为稳定. 这与Bianchi等[17]发现超声浸渍制备的Co/SiO_2催化剂活性、重烃选择性及稳定性较高的结果一致.

Co基催化剂失活的原因较多, 其中硅酸钴的生成是其中之一. Dalai等[33]认为, 随着费托反应的进行, 水分压的升高将导致载体表面高分散的金属Co与载体形成难还原的硅酸钴, 从而造成催化剂失活. 如上文分析, 高功率超声波可以降低浸渍液的pH值, 减弱Co-硅胶相互作用, 而抑制硅酸钴的生成以及金属Co晶粒较小, 在载体上分散度较高, 这些因素都有可能提高催化剂稳定性.

3 结论

在浸渍法制备费托合成Co/Zr/SiO_2催化剂过程中, 施以42 kHz, 有效功率分别为180和210 W的超声波, 浸渍溶液在超声波场中的空化效应可以增大催化剂的比表面积, 减小金属Co的粒径, 提高分散度, 使其较为均匀地分散于载体表面, 其中高功率超声波作用明显. $Co(NO_3)_2$水溶液置于高功率超声波场, 随着超声时间的延长出现$Co(OH)_2$沉淀物, 使得溶液的pH下降; 而Co浸渍液pH值的降低, 可以减弱Co-硅胶相互作用, 从而抑制硅酸钴的生成. 在相同的费托反应条件下, 经高功率超声波处理的Co/Zr/SiO_2催化剂具有较高的分散度和还原度, 因而其活性、C_{5+}选择性和稳定性较高.

参 考 文 献

1 Iglesia E. *Appl Catal A*, 1997, **161**: 59
2 Ernst B, Libs S, Chaumette P, Kiennemann A. *Appl Catal A*, 1999, **186**: 145
3 Khodakov A Y, Chu W, Fongarland P. *Chem Rev*, 2007, **107**: 1692
4 孙予罕, 陈建刚, 王俊刚, 贾丽涛, 侯博, 李德宝, 张娟. 催化学报 (Sun Y H, Chen J G, Wang J G, Jia L T, Hou B, Li D B, Zhang J. *Chin J Catal*), 2010, **31**: 919
5 周从文, 林泉. 神华科技(Zhou C W, Lin Q. *Shen Hua Sci Technol*), 2010, **8**(4): 93
6 吴昊, 胡志海, 聂红, 徐润, 侯朝鹏, 田鹏程, 夏国富(Wu H, Hu Zh H, Nie H, Xu R, Hou Zh P, Tian P Ch, Xia G F). CN 101 863 728. 2009
7 Ali S, Chen B, Goodwin J G Jr. *J Catal*, 1995, **157**: 35
8 Feller A, Claeys M, Van Steen E. *J Catal*, 1999, **185**: 120
9 den Breejen J P, Sietsma J R A, Friedrich H, Bitter J H, Jong K P. *J Catal*, 2010, **270**: 146
10 李廷盛, 尹其光. 超声化学. 北京: 科学出版社 (Li T Sh, Yin Q G. Supersonic Chemistry. Beijing: Sci Press), 1995. 36
11 晏刚, 霍超, 刘化章. 工业催化 (Yan G, Huo Ch, Liu H Zh. *Ind Catal*), 2007, **15**(2): 1
12 刘亮, 于焕良, 邓宝永. 广州化工 (Liu L, Yu H L, Deng B Y. *Guangzhou Chem Ind*), 2009, **37**(3): 31
13 梁新义, 张黎明, 丁宏远, 秦永宁. 物理化学学报 (Liang X Y, Zhang L M, Ding H Y, Qin Y N. *Acta Phys-Chim Sin*), 2003, **19**: 666
14 杨永辉, 林彦军, 冯俊婷, 李殿卿. 催化学报 (Yang Y H, Lin Y J, Feng J T, Evans D G, Li D H. *Chin J Catal*), 2006, **27**: 304
15 刘越男, 吕效平, 韩萍芳. 化工学报 (Liu Y N, Lü X P, Han P F. *J Chem Ind Eng*(*China*)), 2007, **58**: 2805
16 Pirola C, Bianchi C L, Di Michele A, Diodati P, Boffito D, Ragaini V. *Ultrason Sonochem*, 2010, **17**: 610
17 Bianchi C L, Martini F, Ragaini V. *Ultrason Sonochem*, 2001, **8**: 131
18 Mason T J, Lorimer J P. Applied Sonochemistry: Uses of Power Ultrasound in Chemistry and Processing. Weinheim: Wiley-VCH, 2002. 58
19 林仲茂. 清洗世界(Lin Zh M. *Clean World*), 2004, **20**(10): 24
20 Song D Ch, Li J L. *J Mol Catal A*, 2006, **247**: 206
21 Saib A M, Claeys M, Van Steen E. *Catal Today*, 2002, **71**: 395
22 Liu Y Y, Hanaoka T, Miyazawa T, Murata K, Okabe K, Sakanishi K. *Fuel Process Technol*, 2009, **90**: 901
23 张畹徽, 杜尧国, 曹锡章. 无机化学, 下册 (第二版). 北京: 高等教育出版社 (Zhang W H, Du Y G, Cao X Zh. Inorganic Chemistry, Part B. 2nd Ed. Beijing: Higher Educ Press), 1984. 469
24 陈建刚, 相宏伟, 孙予罕. 催化学报 (Chen J G, Xiang H W, Sun Y H. *Chin J Catal*), 2000, **21**: 169
25 Van Steen E, Sewell G S, Makhothe R A, Micklethwaite C, Manstein H, de Lange M, O'Connor C T. *J Catal*, 1996, **162**: 220
26 赵红霞, 朱柘权, 陈建刚, 孙予罕. 催化学报 (Zhao H X, Zhu Zh Q, Chen J G, Sun Y H. *Chin J Catal*), 2004, **25**: 289
27 穆仕芳, 李德宝, 侯博, 陈建刚, 孙予罕. 石油学报 (石油加工)(Mu Sh F, Li D B, Hou B, Chen J G, Sun Y H. *Acta Petrol Sin* (*Petrol Process Sect*)), 2009, (suppl): 5
28 朱柘权, 房克功, 陈建刚, 孙予罕. 燃料化学学报 (Zhu Zh Q, Fang K G, Chen J G, Sun Y H. *J Fuel Chem Technol*), 2005, **33**: 506
29 Kosmulski M. Chemical Properties of Material Surfaces. New York: Marcel Dekker Inc, 2001. 734
30 陈建刚, 相宏伟, 王秀芝, 孙予罕, 刘涛, 胡天斗, 谢亚宁. 催

化学报 (Chen J G, Xiang H W, Wang X Zh, Sun Y H, Liu T, Hu T D, Xie Y N. *Chin J Catal*), 2000, **21**: 359
31 Tauster S J, Fung S C, Baker R T K, Horsley J A. *Science*, 1981, **211**: 1121
32 Ishihara T, Harada K, Eguchi K, Arai H. *J Catal*, 1992, **136**: 161
33 Dalai A K, Davis B H. *Appl Catal A*, 2008, **348**: 1

英 译 文
English Text

With the depletion of crude oil resources and the gradual increase in consumption, many countries are turning to alternative fuels to ensure their energy security. Fischer-Tropsch synthesis (FTS) is one of the most promising ways to convert syngas derived from coal or natural gas into light olefins, gasoline, and diesel. This technology can reduce the dependency on petroleum to a certain extent. Iron- and cobalt-based catalysts have been successfully applied in Sasol's and Shell's commercial plants. Because of the low activity of the water gas shift reaction and the main product being long chain paraffins, cobalt catalysts are promising for the synthesis of heavy hydrocarbons [1–3].

Recently, a large number of domestic achievements have been reported in the development and industrial processing of cobalt-based catalysts such as the cobalt catalyst developed by DICP (Dalian Institute of Chemical Physical, Chinese Academy of Sciences (CAS)), which was used in a pilot project (3000 t/a) in 2007. Their results indicated that the catalyst could run continuously and stably for 5000 h (important achievements in science and technology and advanced special disciplines for DICP 60 years. 2009-02). The two other cobalt catalysts that have been developed by the ICC [4,5] (Institute of Coal Chemistry, CAS) and the RIPP [6] (Research Institute of Petroleum Processing, China Petrochemical Corporation (SINOPEC)) have undergone a long period of experimental evaluation up to 2010. Now, two pilot projects wherein these catalysts are to be used are also in process.

Cobalt catalysts that are supported on silica are mainly prepared by impregnation under normal temperature and pressure conditions. Zirconium promotion has been widely used in silica supported catalysts, and this results in higher FTS reaction rates and an increase in C_{5+} selectivity. This promotion can prevent the interaction between cobalt particles and the support and thus the formation of hardly reducible cobalt silicates [3]. However, Co_3O_4 crystallites tend to agglomerate on the support during catalyst drying or calcination and, therefore, the degree of dispersion of the metallic cobalt will decrease. The size and distribution of the cobalt crystallites on the support influence the catalytic activity and stability [7–9]. Therefore, research is currently focused on improving the degree of dispersion of the active sites on the $Co/Zr/SiO_2$ catalyst surface.

During incipient wetness impregnation, the support and the impregnation solution are all exposed to an ultrasonic environment. Cavitation bubbles can be formed in solution and they are released under this extreme high temperature and high pressure environment. Active components are loaded onto the support when these bubbles collapse [10]. In addition, ultrasonic oscillation facilitates an even distribution of the active components [11,12]. In contrast to the catalysts prepared by normal impregnation, it has been reported [13–15] that in an ultrasonic environment the sizes of the active metals were smaller and the metal particles were more evenly dispersed on γ-Al_2O_3 surfaces. This results in an improvement in the activity and stability of the catalysts. In addition, Pirola et al. [16] and Bianchi et al. [17] respectively loaded metallic iron and cobalt onto silica supports in an ultrasonic environment. They concluded that the catalysts gave a high degree of dispersion and high conversion of carbon monoxide.

General speaking, the cavitation and intensity of ultrasound with a certain frequency are enhanced with an increase in ultrasonic power [10]. With an increase in impregnation pressure air tends to dissolve into the impregnation solution causing the cavitation threshold to drop. On the other hand, with a collapse of cavitation bubbles an increase in the gaseous components in solution will decrease the intensity of the blast wave [10,18]. According to the principle of ultrasound-vacuum cleaning [19], if the support and the impregnation solution are vacuum-treated in degassing units the impregnation process in an ultrasonic environment can be intensified.

Currently, few reports exist about the preparation of cobalt catalysts in an ultrasound-vacuum environment. This study is expected to improve the dispersion of metallic cobalt on silica surfaces using this method. In this paper, we focused on the preparation of a $Co/Zr/SiO_2$ catalyst using the ultrasound-vacuum method and we investigated the effects of different ultrasonic power on catalyst morphology, the size of cobalt particles, the degree of dispersion/reduction, and the catalytic activity toward the FTS. In addition, N_2 physisorption, X-ray diffraction (XRD), transmission electron microscopy (TEM), H_2 temperature-programmed desorption (H_2-TPD), and H_2 temperature-programmed reduction (H_2-TPR) were used to characterize the catalysts.

1 Experimental

1.1 Preparation of the catalysts

The silica support (Sino-pharm Chemical Reagent Co., Ltd) was put into an ultrasonic generator (Branson Ultra-

sonics Corp, ultrasonic frequency 42 kHz, effective power 180 and 210 W). By incipient wetness impregnation, a 5% $Zr(NO_3)_4$ (AR, Sino-pharm Chemical Reagent Co., Ltd) aqueous solution was dripped onto the support at –0.1 MPa. The ultrasonic generator was switched on and its power was regulated at 210 W (or 180 W). The sample was treated under these ultrasonic-vacuum conditions for 1 h. After the catalyst precursor was dried at 383 K for 12 h it was impregnated with a 20% $Co(NO_3)_2$ (AR, Sino-pharm Chemical Reagent Co., Ltd) aqueous solution at –0.1 MPa and was then treated by ultrasound at 210 W (or 180 W) for 1 h. The catalyst was dried at 383 K for 12 h and calcined at 673 K for 6 h. Catalyst particles of 60–80 mesh were evaluated for the FTS reaction after they were crushed, and sieved. The catalysts that were prepared by the above procedures are denoted 20%Co/5%Zr/SiO_2(H) and 20%Co/5%Zr/SiO_2(L), where H and L refer to higher and lower ultrasound power. In addition, the 20%Co/5%Zr/SiO_2 (V) catalyst was also prepared using the above procedures but without ultrasonic treatment.

The 20% $Co(NO_3)_2$ and 5% $Zr(NO_3)_4$ aqueous solutions were simultaneously put into the ultrasonic generator. We determined the change in solution pH with a change in ultrasonic power and treatment time. A pH meter (Model: PHSJ-3F, resolution: 0.01, Shanghai Precision & Scientific Instrument Co., Ltd) was used to measure the pH of the solution. Before the pH meter was used, it was calibrated using two buffer solutions with pH values of 4.0 and 7.0.

1.2 Characterization of the catalysts

The BET surface area, pore size distribution and pore volume were measured by N_2 physisorption using a Micromeritics ASAP 2010 instrument. XRD measurements were carried out using the Cu K_α radiation of a Bruker D8-ADVANCE powder diffractometer (40 kV, 40 mA and 4°/min). The H_2-TPR experiment was carried out using a Micromeritics Autochem II 2920. 50 mg samples were used for programmed-reduction in a 10% H_2–90% Ar mixed gas at a rate of 10 K/min from ambient temperature to 1073 K. The H_2-TPD experiment was performed using a self-made device. Before the experiment, the 50 mg samples were reduced using high purity H_2 at 673 K for 5 h. After they were cooled to room temperature, high purity N_2 at a flow rate of 30 ml/min was passed over the catalysts for 1 h. The temperature was then increased from ambient temperature to 1073 K at 10 K/min. The TEM images were obtained using a FEI Tecnai 20 S-TWIN instrument.

1.3 Activity test for the FTS

The Fischer-Tropsch synthesis was performed in a fixed-bed reactor (φ = 8 mm). The catalyst was reduced in situ with H_2 at 673 K and under atmospheric pressure for 12 h. After reduction, the reactor was cooled to room temperature. Syngas was introduced to the reactor and the pressure was gradually increased to the set value. Meanwhile, the reactor temperature was increased to the set value at 2 K/min. When the steady state was reached after an initial reaction of 12 h we calculated the carbon monoxide conversion and the selectivity of products under the different reaction conditions. The effluent gas was passed through an Agilent 6890(N) GC for online analysis. Liquid product analysis was performed using an Agilent 6820 GC equipped with an FID detector.

2 Results and discussion

2.1 Structural properties of the catalysts

The textural properties and cobalt particle size of the different Co/Zr/SiO_2 catalysts are showed in Table 1. The BET surface area, pore volume, and average pore diameter of the silica support decreases sharply with component load. However, when the 20%Co/5%Zr/SiO_2(H) catalyst was treated with higher power ultrasound its BET surface area was found to be relatively larger. This result is consistent with that reported previously [13–16].

In addition, no zirconium phase was detected in the XRD patterns of the three fresh catalysts (not shown here), which indicates that zirconia is highly dispersed on the silica support [7]. According to literature [20–22], the average diameter of the Co_3O_4 crystallites can be calculated using the Scherrer equation from the most intense Co_3O_4 peak at 2θ = 36.9°. The size of metallic cobalt and the degree of dispersion were determined using the formulae: $d = 0.75 \times d(Co_3O_4)$ and $D(\%) = 96/d$. The calculated results are shown in Table 1. The size of metallic cobalt in the 20%Co/5%Zr/SiO_2(H) catalyst is at a minimum and, on the contrary, its degree of dispersion is at a maximum.

TEM was conducted to study the surface morphology of the three calcined catalysts. As Fig. 1 shows, it is obvious that the cobalt particles of 20%Co/5%Zr/SiO_2(V) are cluttered. However, the cobalt particles of 20%Co/5%Zr/SiO_2(H) are more uniform and nebulous, which implies that the cobalt particles are smaller and are highly dispersed on the support. This phenomenon is similar to that obtained by Liang et al. [13] who reported that $LaCoO_3$ was evenly distributed on a γ-Al_2O_3 support in an ultrasonic environment. The impregnation solution can create cavitation bubbles in the ultrasonic environment at –0.1 MPa. As Fig. 1(d) shows, the surface of the 20%Co/5%Zr/ SiO_2(H) catalyst shows that many cavity traces were eroded by the cavitation bubbles.

2.2 Solution pH in an ultrasonic environment

The pH of the impregnation solution can change when the solution is put into an ultrasound environment at extremely high temperature and high pressure. Table 2 shows the pH values of the 20% $Co(NO_3)_2$ and the 5% $Zr(NO_3)_4$ aqueous solutions upon changing the ultrasonic power and the treatment time. The pH values of the two solutions decrease dramatically in the higher power ultrasonic environment. Furthermore, when a 20% $Co(NO_3)_2$ aqueous solution is treated with higher power ultrasound for 1 h, pink $Co(OH)_2$ precipitation occurs. This is due to more $H^{\bullet}$ and $OH^{\bullet}$ free radicals being present in the aqueous solution when the solution is treated with high intensity ultrasound [10]. The $Co(H_2O)_6^{2+}$ ions react with $OH^{\bullet}$ and precipitation occurs, which leads to the pH of the impregnation solution decreasing ($Co(H_2O)_6^{3+}$ ions cannot exist in the aqueous solution because of their high oxidation state [23]). However, lower-intensity ultrasound decreases the pH of the solution slightly.

Chen et al. [24] reported that $Co(H_2O)_6^{2+}$ ions can interact with silanol groups on the surface of silica during the impregnation process. Silica is an amphoteric material and the different kinds of silanol groups depend on the pH of the impregnated solution and they exist as Si–OH, SiO^-, or $SiOH_2^+$. Van Steen et al. [25] reported that the interaction between $Co(H_2O)_6^{2+}$ ions and silanol groups becomes stronger as the pH increases in the impregnation solution; in addition, water ligands were necessary for the formation of a surface cobalt silicate. It has also been reported that the pH of an impregnation solution affects the Co-silica interaction [26–28]. When the pH is less than the isoelectric point of silica (2.0–3.5 [29]), a surplus of positive charge is present on the surface of the silica. Because of an electrostatic interaction the direct adsorption of negative nitrate ions takes place and the $Co(H_2O)_6^{2+}$ ions are in indirect contact with the silanol groups, which helps to weaken the Co-silica interaction, inhibit formation of cobalt silicates, and improve the degree of reduction of the catalyst. Higher power ultrasound can decrease the pH of the impregnation solution. Theoretically, it will help weaken the Co-silica interaction and finally inhibit the formation of cobalt silicates. Of course, this hypothesis should be validated by other characterization techniques.

2.3 Result of H_2-TPD

The H_2-TPD profiles of the different $Co/Zr/SiO_2$ catalysts are shown in Fig. 2. According to literature [30], the hydrogen desorption peak at low temperature (about 463 K) is due to hydrogen spillover from metallic cobalt to the support. The other desorption peaks at medium (about 603 K) and high temperature (about 703 K) respectively relate to hydrogen desorption over the metallic cobalt on zirconia and the silica surface. From Fig. 2, when the $Co/Zr/SiO_2$ catalysts are treated with ultrasound the peaks at about 463 K move to the low temperature direction and hydrogen adsorption decreases. Higher power ultrasound causes the hydrogen desorption peak on the silica surface to move to the low temperature direction and causes the amount of hydrogen adsorption on the zirconia and silica surfaces to increase (content of hydrogen adsorption is calculated on the basis of the H_2-TPD integrated area from 489 to 803 K. 20%Co/5%Zr/SiO_2(H) > 20%Co/5%Zr/SiO_2(L) > 20%Co/5%Zr/SiO_2(V)).

The strong-metal-support-interaction (SMSI), as Tauster et al. [31] explained, is produced by the electron transfer from the reduced oxide support to the metal particle. Therefore, hydrogen chemisorption on the metal is essentially reduced. Ishihara et al. [32] reported that when metallic ruthenium was loaded onto a silica support the catalyst showed higher catalytic activity for the FTS. Further research indicated that an electron is transferred from the metal particle to the support, which decreases the electron density of metallic ruthenium. The corresponding hydrogen desorption peak (characterized by H_2-TPD) moves to the low temperature direction. As for the 20%Co/5%Zr/SiO_2(H) catalyst, the hydrogen desorption peak at about 703 K that moves to the low temperature direction can be explained in terms of electron transfer from metallic cobalt to the silica support and a decrease in electron density of the metallic cobalt. Therefore, the Co-silica interaction will be weakened and the amount of hydrogen that adsorbs on the support will increase. Additionally, a larger amount of small cobalt crystallites are present on the 20%Co/5%Zr/SiO_2(H) catalyst and hydrogen can be adsorbed, dissociated, and transferred to the catalyst's surface at lower temperature (about 450 K). This also facilitates the adsorption of hydrogen which further promotes the FTS. Considering the peak at about 603 K, ultrasound slightly influenced hydrogen adsorption over metallic cobalt on the surface of zirconia, which is perhaps related to the low content of zirconia in these catalysts.

2.4 Results of H_2-TPR

The H_2-TPR profiles are shown in Fig. 3 for the different $Co/Zr/SiO_2$ catalysts. Generally speaking, the reduction process of the cobalt catalyst that was supported on silica is divided into two steps: Co_3O_4 (with trivalent cobalt oxides and bivalent cobalt oxides) → CoO → Co^0. Moreover, from 703–1003 K there is a hidden reduction of the barely reducible cobalt silicate [2,25]. As Fig. 3(a) shows, the Co_3O_4 reduction peak of the 20%Co/5%Zr/SiO_2(H) catalyst becomes inconspicuous, which is due to the less trivalent and more bivalent cobalt oxides being present in the Co_3O_4 crystallites. In addition, the figure also implies that a single phase of bivalent cobalt oxides is present because the CoO

reduction peak is sharper [26]. The reductive behavior of the 20%Co/5%Zr/ SiO_2(H) catalyst that was prepared in the higher-power ultrasonic environment might be relevant to $Co(OH)_2$ precipitation. In addition, the cobalt silicate reduction peak of the 20%Co/5%Zr/SiO_2(H) catalyst becomes more inconspicuous, which means that higher power ultrasound can weaken the interaction between the cobalt crystallites and the silica support to form less cobalt silicate.

By combining the results of H_2-TPD and H_2-TPR, we conclude that higher power ultrasound can weaken the Co-silica interaction, enhance the degree of cobalt particle reduction (see Table 1) and increase the content of hydrogen adsorption on the catalyst. However, since the pH of the impregnation solution in the lower power ultrasonic environment changes slightly, the Co-silica interaction and the cobalt silicates still exist.

2.5 Catalytic activity toward the FTS

The performance of the three $Co/Zr/SiO_2$ catalysts at different temperatures and with other reaction conditions of 2 MPa, $H_2/CO = 2.0$ and GHSV = 1000 h^{-1} is listed in Table 3. Iglesia [1] reported that if the size of the metallic cobalt was more than 6 nm, the FTS was a reaction of structure insensitivity. Moreover, it has been found that higher volumetric cobalt site densities on the catalyst leads to a higher FTS reaction rate and better selectivity for C_{5+} products. The higher power ultrasound is conducive to the dispersion of smaller cobalt particles on the support and it also leads to a decrease in the pH of the $Co(NO_3)_2$ impregnation solution. When the pH is less than the isoelectric point of silica, a surplus of positive charge is present on the silica surface. Because of the electrostatic interaction, nitrate ions are directly adsorbed on the support and the $Co(H_2O)_6^{2+}$ ions are in indirect contact with the silanol groups, which helps to weaken the Co-silica interaction and inhibit the formation of cobalt silicates as well as improve both the degree of reduction and the active sites in the 20%Co/5%Zr/SiO_2(H) catalyst.

In addition, from the result of H_2-TPD, hydrogen can be adsorbed, dissociated, and transferred to the 20%Co/5%Zr/SiO_2(H) catalyst surface at lower temperature, which also facilitates the FTS. Therefore, under the same reaction conditions the 20%Co/5%Zr/SiO_2(H) catalyst has the highest catalytic activity and selectivity for C_{5+}. After a reaction over 48 h and at 493 K, the three catalysts were deactivated to a different extent. In contrast, the 20%Co/5%Zr/SiO_2(H) catalyst is more stable, which is consistent with Bianchi et al. [17] who reported on the stability of the Co/SiO_2 catalyst that was treated by ultrasound.

There are many reasons for the deactivation of cobalt-based catalysts. Dalai et al. [33] postulated that cobalt silicate formation was one reason because of the increase in water concentration with time-on-stream (TOS) in the FTS. Higher power ultrasound can change the catalyst morphology, weaken the Co-silica interaction and inhibit the formation of cobalt silicates. These factors may assist in improving the stability of the 20%Co/5%Zr/SiO_2(H) catalyst.

3 Conclusions

During incipient wetness impregnation, a $Co/Zr/SiO_2$ catalyst for the Fischer-Tropsch synthesis was prepared in a 42 kHz ultrasonic environment. The cavitation that was created by ultrasound with higher power (210 W) or lower power (180 W) increased the BET surface area of the catalyst and evenly distributed the smaller cobalt crystallites over the support. The textural properties and the size of the cobalt particles change obviously for the catalyst treated with higher power ultrasound. Moreover, pink $Co(OH)_2$ precipitation appeared in the cobalt nitrate aqueous solution and the pH of the solution decreased simultaneously with an increase in the higher power ultrasound treatment time. When the pH of the impregnation solution was less than the isoelectric point of silica, the $Co(H_2O)_6^{2+}$ ions were in indirect contact with the silanol groups, which helped to weaken the Co-silica interaction and inhibit the formation of cobalt silicate. Under the same FTS reaction conditions, the activity and stability of the 20%Co/5%Zr/SiO_2(H) catalyst were superior to that of the others because of its higher dispersion and degree of reduction.

Full-text paper available online at Elsevier ScienceDirect
http://www.sciencedirect.com/science/journal/18722067